SUPPLEMENTARY MATERIALS - DEVUDP

Anonymous authors
Paper under double-blind review

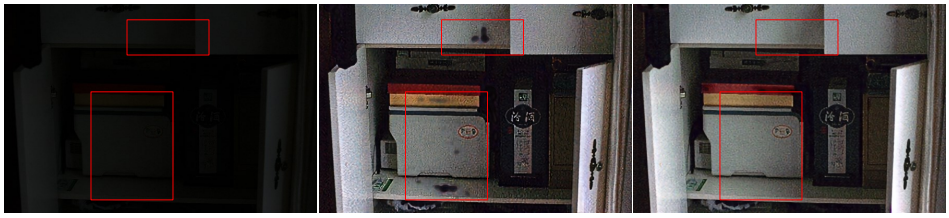

Low-light T-branch only T-branch & S-branch

Figure 1: Visual ablation studies for S-branch. As can be seen, S-branch helps to remove the artifacts and noise in the processed results.

Table 1: Quantitative ablation studies on three tasks, i.e., deblurring on GoPro (Nah et al., 2017), LLIE on LOL (Wei et al., 2018) and mixed degradation processing on LOL-Blur (Zhou et al., 2022).

Line	Methods	GoPro	LOL	LOL-Blur	Average
1	w/o S-branch	22.02/0.695	16.29/0.607	18.23/0.645	18.85/0.649
2	w/o downsizing	22.12/0.718	15.48/0.636	18.12/0.660	18.57/0.672
3	DEvUDP	22.19/0.708	16.88/0.667	18.03/0.653	19.03/0.676

1 USED DATASETS

The detailed information of used datasets is as follows:

- **GoPro (*blur*) (Nah et al., 2017).** The most widely-used dataset for motion deblurring. It consists of 2103 blurry-sharp images pairs for training and 1111 pairs for inference. The resolution of each image is 1280× 720. The blurry frame of GoPro is obtained by averaging the multiple shape frames, and strictly speaking, it is a synthetic dataset.
- **RealBlur-J (*blur*) (Rim et al., 2020).** It includes 3758 real-world training pairs and 980 inference pairs. The resolution of the image is not mixed, and we resize the image uniformly to 640×720. It is a real-world blur dataset.
- **LOL (*low-light*) (Wei et al., 2018).** The most widely-used real-world dataset for low-light image enhancement (LLIE). It includes 485 low-high light image pairs for training and 15 pairs for inference. The resolution of each image is 640× 400.
- **LOL-Blur (*mixed blur & low-light*) (Zhou et al., 2022).** The first large-scale dataset for mixed deblurring & low-light processing. It consists of 12000 low-blurry/high-sharp image pairs, in which 10200 pairs are used for training and 1800 pairs for inference. The resolution of each image is 1120× 640. It is a synthetic dataset since all images are synthesized by a specific pipeline.
- **Rain100H (*rain*) (Yang et al., 2017).** One of the widely-used difficult deraining datasets. It consists of 1800 rain/rain-free image pairs for training and 100 pairs for inference. The resolution of each image is either 481× 321 or 321× 481. It is a synthetic dataset.
- **Rain100H-Dark (*mixed rain & low-light*).** The dataset we constructed for mixed rain & low-light processing. Specifically, we select the images in Rain100H as basic data and follow the widely-used low-light synthesis pipeline (Lv et al., 2021) to simulate mixed degradation.

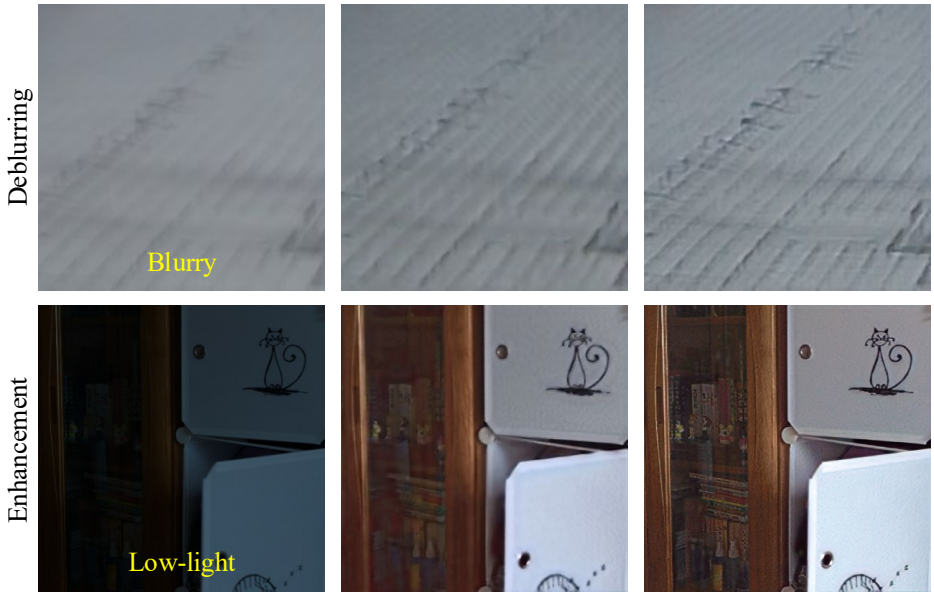

Figure 2: Visual ablation studies for downsizing operation on deblurring and low-light image enhancement tasks. As can be seen, the downsizing operator makes the processed results sharper.

Table 2: Quantitative comparison of deraining performance on widely-used deraining dataset Rain100H (Yang et al., 2017).

Methods	PSNR↑	SSIM↑	MAE↓	LPIPS↓
SIRR	20.64	0.656	20.26	0.321
Semi-Deraingan	20.66	0.754	20.20	0.244
CycleGAN	22.82	0.740	14.48	0.202
DerainCycleGAN	19.96	0.678	22.23	0.324
NLCL	17.04	0.585	33.02	0.275
DEvUDP (Ours)	23.09	0.743	13.73	0.181

Table 3: Quantitative comparison of LLIE performance on LOL (Wei et al., 2018) dataset.

Methods	PSNR↑	SSIM↑	MAE↓	LPIPS↓
LIME	14.22	0.514	50.92	0.368
Zhang et al.	14.02	0.513	51.91	0.372
Zero-DCE	14.97	0.500	41.62	0.432
Zero-DCE++	14.80	0.516	43.72	0.413
RUAS	16.40	0.500	39.11	0.270
SCI	14.02	0.508	52.36	0.388
DEvUDP (Ours)	16.02	0.668	39.20	0.320

2 Ablation Studies

1) Effectiveness of S-branch. To verify the effectiveness of S-branch, we conduct quantitative and visual ablation studies on related three tasks, i.e., deblurring on GoPro (Nah et al., 2017), low-light image enhancement on LOL (Wei et al., 2018) and mixed degradation processing on LOL-Blur (Zhou et al., 2022) . The line 1 and 3 in Table 1 quantitatively proves the effectiveness of S-branch. Besides, Fig.1 shows that the S-branch is indispensable for the whole architecture.

2) Effectiveness of downsizing operation. Before all data augment operation, the image should be downsized while keeping the width-high ratio unchanged. To verify the effectiveness of this downsizing operation, we quantitatively and qualitatively compare the performance on above tasks before and after removing the downsizing operation. The line 2 and 3 in Table 1 demonstrate the gain of the downsizing operator in quantitative performance, and Fig.2 shows that the downsizing operation can make the processed results more clear.

3 Extension Experiments, Potential Limitation and Discussion

There are always two sides to a coin and our DEvUDP may have potential limitations. Compared to other joint task processing strategies (i.e., ODPI, AiO and MDPI), our DEvUDP is specifically applicable to the task of joint deblurring and LLIE, which is determined by the characteristics of the tasks themselves. Perhaps joint LLIE and other IRAE task is also feasible (e.g., enhancing

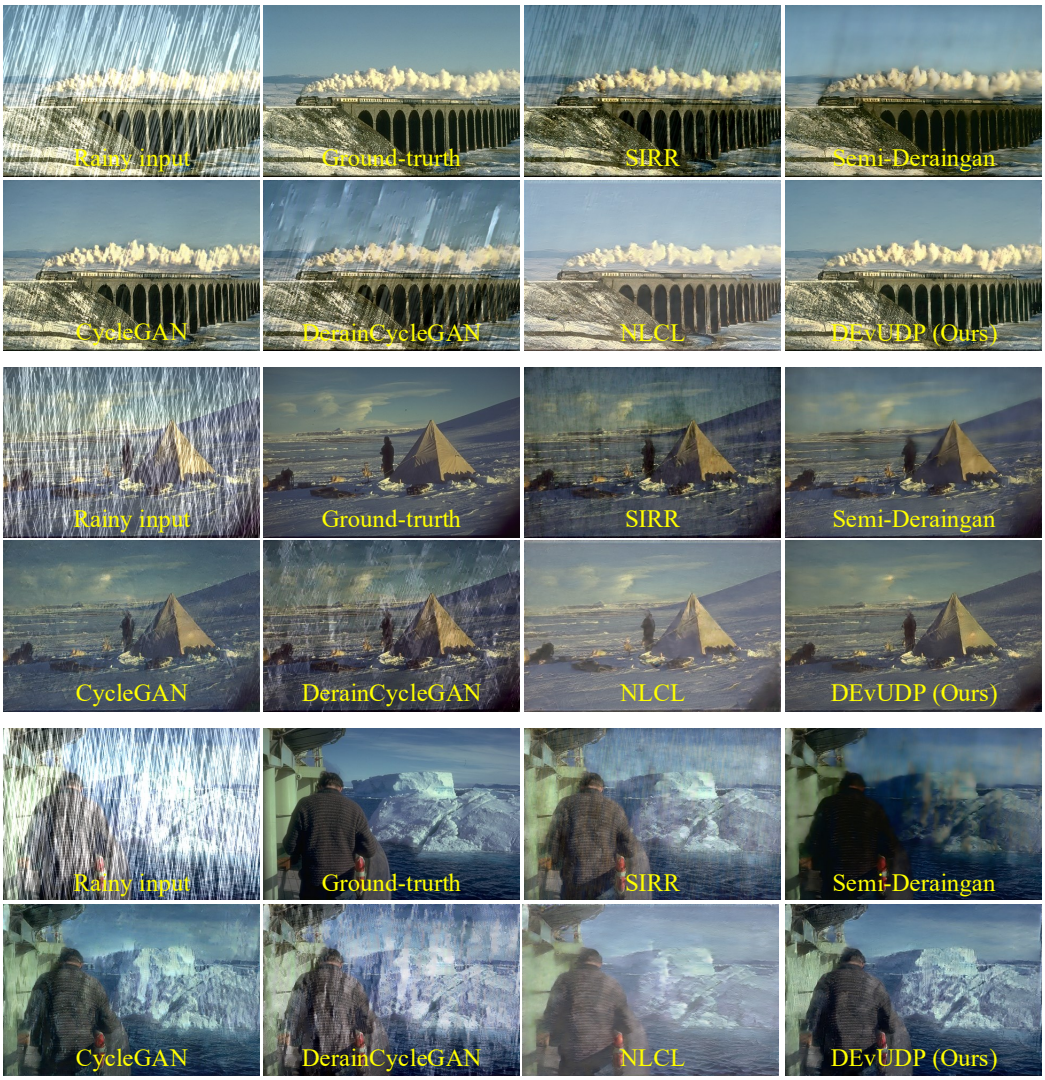

Figure 3: Visualization comparison between our method and several unsupervised/semi-supervised methods. From left-top to right-bottom: rainy input, ground-truth, SIRR (Wei et al., 2019), Semi-Deraingan (Wei et al., 2021b), CycleGAN (Zhu et al., 2017), DerainCycleGAN (Wei et al., 2021a), NLCL (Ye et al., 2022) and Ours. As can be seen, our DEvUDP has better visual effect.

an image via deraining paradigm), but at least the LLIE task is a necessity. In fact, we did this. Like joint deblurring and LLIE, we conduct the experiment on joint deraining and LLIE using the same architecture and experimental settings. For dataset selection, we choose one of widely-used difficult datasets Rain100H (Yang et al., 2017) for deraining, the most widely-used LOL (Wei et al., 2018) dataset for LLIE and synthetic dataset Rain100H-Dark for mixed degradation processing. We first use the training set of Rain100H for training and use the test sets of Rain100H and LOL for inference.

For the task of deraining, we employ two semi-supervised methods (i.e., SIRR (Wei et al., 2019) and Semi-Deraingan (Wei et al., 2021b)) and two unsupervised methods (i.e., CycleGAN (Zhu et al., 2017), DerainCycleGAN (Wei et al., 2021a) and NLCL (Ye et al., 2022)) for comparison. The quantitative and qualitative results are shown in Table 2 and Fig.3. From the results, we can learn that: 1) Our method also performs well for deraining although it is specifically designed for joint deblurring & LLIE, since Rain100H is a relatively difficult dataset; 2) Our method obtains higher numerical results while achieving more visually pleasing results.

Figure 4: Visualization comparison between our method and several optimizing-based/zero-reference data-based methods. From left-top to right-bottom: low-light input, ground-truth, LIME (Guo, 2016), Zhang et al. (Zhang et al., 2019), Zero-DCE (Guo et al., 2020), RUAS (Liu et al., 2021), SCI (Ma et al., 2022) and Ours. Clearly, the enhanced results of our DEvUDP are more natural.

Low-light & rainy input | Processed result | Ground-truth

Figure 5: Visualization result of our method for mixed rain & low-light processing.

For the task of LLIE, we directly use the model pre-trained on the deraining dataset Rain100H (Yang et al., 2017) for LLIE. Six related methods (i.e., LIME (Guo, 2016), Zhang et al. (Zhang et al., 2019), Zero-DCE (Guo et al., 2020), Zero-DCE++ (Li et al., 2022), RUAS (Liu et al., 2021) and SCI (Ma et al., 2022)) are involved in the experimental comparison and the results are demonstrated in Table 3 and Fig.4. From the results, we can learn that: 1) the model pre-trained by deraining dataset could also have the ability to enhance the low-light image, not only applicable for deblurring dataset; 2) The quantitative result of our method is competitive and the visualization result is quite natural comparing to other methods.

For the mixed processing of rain & low-light, we also try to use the model pre-trained on the deraining dataset Rain100H (Yang et al., 2017) to recover the corrupted image. The visualization result are displayed in Fig.5. From the figure, we can see that the visual effect of the processed result doesn't look so good. Specifically, the rain streaks are not well removed and there is no visible enhancement effect.

We speculate that the possible reasons for this problem are as follows: 1) The model may not adaptable to the joint deraining and LLIE since the deblurring setting was adopted directly, which means that this problem might be solved if we could find a more suitable model and setting; 2) The self-regression technique helps adjust global brightness, which means that it can adjust under- or over-exposed images to be normal based on global statistical information (e.g., the average of three-channel of the whole image). However, the rain streaks themselves can be seen as an overexposed property, globally neutralising the low-light and causing the rainy low-light image itself to fall into the normal range.

In summary, we have demonstrated, at least experimentally, that it is applicable to enhance low-light images using other IRAE paradigm, and that the ability of mixed degradation processing in the proposed strategy needs to be further investigated and improved.

REFERENCES

Chunle Guo, Chongyi Li, Jichang Guo, Chen Change Loy, Junhui Hou, Sam Kwong, and Runmin Cong. Zero-reference deep curve estimation for low-light image enhancement. In *Proceedings of the IEEE/CVF Conference on Computer Vision and Pattern Recognition (CVPR), Seattle, WA, USA*, pp. 1777–1786, 2020.

Xiaojie Guo. LIME: A method for low-light image enhancement. In *Proceedings of the International Conference on Multimedia (ACM MM), Amsterdam, The Netherlands*, pp. 87–91, 2016.

Chongyi Li, Chunle Guo, and Chen Change Loy. Learning to enhance low-light image via zero-reference deep curve estimation. *IEEE Trans. Pattern Anal. Mach. Intell (TPAMI).*, 44(8):4225–4238, 2022.

Risheng Liu, Long Ma, Jiaao Zhang, Xin Fan, and Zhongxuan Luo. Retinex-inspired unrolling with cooperative prior architecture search for low-light image enhancement. In *Proceedings of the IEEE Conference on Computer Vision and Pattern Recognition (CVPR), virtual*, pp. 10561–10570, 2021.

Feifan Lv, Yu Li, and Feng Lu. Attention guided low-light image enhancement with a large scale low-light simulation dataset. *Int. J. Comput. Vis.*, 129(7):2175–2193, 2021.

Long Ma, Tengyu Ma, Risheng Liu, Xin Fan, and Zhongxuan Luo. Toward fast, flexible, and robust low-light image enhancement. In *Proceedings of the IEEE/CVF Conference on Computer Vision and Pattern Recognition (CVPR), New Orleans, LA, USA*, pp. 5627–5636, 2022.

Seungjun Nah, Tae Hyun Kim, and Kyoung Mu Lee. Deep multi-scale convolutional neural network for dynamic scene deblurring. In *Proceedings of the IEEE Conference on Computer Vision and Pattern Recognition (CVPR), Honolulu, HI, USA*, pp. 257–265, 2017.

Jaesung Rim, Haeyun Lee, Jucheol Won, and Sunghyun Cho. Real-world blur dataset for learning and benchmarking deblurring algorithms. In *Proceedings of the Computer Vision - 16th European Conference (ECCV), Glasgow, UK*, volume 12370, pp. 184–201, 2020.

Chen Wei, Wenjing Wang, Wenhan Yang, and Jiaying Liu. Deep retinex decomposition for low-light enhancement. In *Proceedings of the British Machine Vision Conference (BMVC), Newcastle, UK*, pp. 155, 2018.

Wei Wei, Deyu Meng, Qian Zhao, Zongben Xu, and Ying Wu. Semi-supervised transfer learning for image rain removal. In *Proceedings of the IEEE Conference on Computer Vision and Pattern Recognition (CVPR), Long Beach, CA, USA*, pp. 3877–3886, 2019.

Yanyan Wei, Zhao Zhang, Yang Wang, Mingliang Xu, Yi Yang, Shuicheng Yan, and Meng Wang. Deraincyclegan: Rain attentive cyclegan for single image deraining and rainmaking. *IEEE Trans. Image Process (TIP).*, 30:4788–4801, 2021a.

Yanyan Wei, Zhao Zhang, Yang Wang, Haijun Zhang, Mingbo Zhao, Mingliang Xu, and Meng Wang. Semi-deraingan: A new semi-supervised single image deraining. In *Proceedings of the IEEE International Conference on Multimedia and Expo (ICME), Shenzhen, China*, pp. 1–6, 2021b.

Wenhan Yang, Robby T. Tan, Jiashi Feng, Jiaying Liu, Zongming Guo, and Shuicheng Yan. Deep joint rain detection and removal from a single image. In *Proceedings of the IEEE Conference on Computer Vision and Pattern Recognition (CVPR), Honolulu, HI, USA*, pp. 1685–1694, 2017.

Yuntong Ye, Changfeng Yu, Yi Chang, Lin Zhu, Xi-Le Zhao, Luxin Yan, and Yonghong Tian. Unsupervised deraining: Where contrastive learning meets self-similarity. In *Proceedings of the IEEE/CVF Conference on Computer Vision and Pattern Recognition (CVPR), New Orleans, LA, USA*, pp. 5811–5820, 2022.

Qing Zhang, Yongwei Nie, and Wei-Shi Zheng. Dual illumination estimation for robust exposure correction. *Comput. Graph. Forum*, 38(7):243–252, 2019.

Shangchen Zhou, Chongyi Li, and Chen Change Loy. Lednet: Joint low-light enhancement and deblurring in the dark. In *Proceedings of the Computer Vision - 17th European Conference (ECCV), Tel Aviv, Israe*, volume 13666, pp. 573–589, 2022.

Jun-Yan Zhu, Taesung Park, Phillip Isola, and Alexei A. Efros. Unpaired image-to-image translation using cycle-consistent adversarial networks. In *Proceedings of the IEEE International Conference on Computer Vision (ICCV), Venice, Italy*, pp. 2242–2251, 2017.